



Stress line additive manufacturing (SLAM) for 2.5-D shells

Kam-Ming Mark TAM^{1*}, James R. COLEMAN², Nicholas W. FINE¹, Caitlin T. MUELLER¹

^{1*} Massachusetts Institute of Technology
77 Massachusetts Avenue, MIT Room 5-418, Cambridge, MA 02139, United States
kmmt@mit.edu

² Singapore University of Technology and Design

Abstract

In the field of digital fabrication, additive manufacturing (AM, sometimes called 3D printing) has enabled the fabrication of increasingly complex geometries, though the potential of this technology to convey both geometry and structural performance remains unmet. Typical AM processes produce anisotropic products with strength behavior that varies according to filament orientation, thereby limiting its applications in both structural prototypes and end-use parts and products (Mueller *et al.* [1]). The paper presents a new integrated software and hardware process that reconsiders the traditional AM technique of fused deposition modelling (FDM) by adding material explicitly along the three-dimensional principal stress trajectories, or stress lines, of 2.5-D structural surfaces. As curves that indicate paths of desired material continuity within a structure, stress lines encode the optimal topology of a structure for a given set of design boundary conditions. The use of a 6-axis industrial robot arm and a heated extruder, designed specifically for this research, provides an alternative to traditional layered manufacturing by allowing for oriented material deposition. The presented research opens new possibilities for structurally performative fabrication.

1. Introduction

1.1 Additive manufacturing and fused-deposition modelling

Over the last two decades, developments in the fields of computational design and digital fabrication have provided tools for architects and designers the tools to rapidly generate an initial prototype from concept through additive manufacturing (AM). Conventional AM methods include stereolithography (SLA), fused-deposition modeling (FDM), and selective laser sintering (SLS), as implemented in popular commercial 3d printing systems developed by companies such as Stratasys, Formlabs, MakerBot Industries and 3D Systems. In today's market, consumer- and designer- grade AM products are largely based on FDM, or the similar technology of fused filament fabrication (FFF), due to the lower purchasing and maintenance costs of these systems [2]. With the popularization of consumer 3D-printer, AM processes have become accessible to designers; it is now an indispensable design tool that permits complex geometrical and formal exploration in conceptual architectural design.

Beyond its application as scaled representation of full scale design ideas, the application of AM techniques to the fabrication of full scale structures is also under investigation by researchers and designers. High-profile design projects in full-scale additive manufacturing have come from a diverse group of designers ranging from mass-production-oriented system designers like Contour Crafting [3], to local practices such as the Amsterdam-based DUS, who are in the process of fabricating a traditional, full-scale “canal house” using FDM [4].

1.2 Anisotropic limitation and alternative proposal

Although recent large-scale implementations of additive manufacturing technologies have generated considerable excitement over the technology’s future role within the field of building technology, there are a still number of challenges intrinsic to the basic premise of FDM and related techniques that remain unresolved. Fundamentally, recent developments have not radically altered the 3-axis layer-based paradigm of the conventional printing technique that is known to reduce the structural strength of fabricated objects. In typical FDM processes, material is deposited in a criss-cross pattern in layers parallel to the horizontal printing bed, which leads to anisotropic structural elements with strength and ductility properties that vary significantly depending on the orientation of the applied forces: existing research has shown that the tensile capacity of specimens loaded perpendicular to filament orientation can be up to 50% weaker than a specimen loaded in parallel, because the weak fusion between horizontal layers provides a natural weak point for breakage (Mueller *et al.* [1]). This anisotropy negatively affects the durability of the printed specimen, and limits the end-use application of additive manufacturing technologies, such that AM technologies have failed to become a meaningful digital fabrication technique that can convey both physical performance and architectural geometry.

Since the structural challenges of conventional additive manufacturing techniques are attributed to the limited capacity for the extruder to achieve varied orientations, this paper proposes an alternative approach to filament extrusion that combines multi-axis robot machining to allow for oriented filament deposition, similar to recent implementation of free-form 3D printing such as those developed by the Joris Laarman Lab [5]. Specifically, this paper proposes filament alignment to major lines of axial forces, as indicated by a structural-pattern-based analytical framework known as principal stress lines.

2. Structural patterns and principal stress lines

Structural patterns are materialized integrations of stress vectors over each infinitesimal element that comprises an investigated structural body. For principal stress lines, vector orientations are determined by stress transformations of stress components in each of these elements to their equivalent stress components at their respective principal stress planes, which correspond to the internal element orientation in which the shear stress components vanish and the normal stress components are at maximum. Structural designers are interested in principal stress lines because they provide a visualization of the natural force flow of an applied load on the system, which shows the lines of desirable material continuity for a given design domain (Michalatos and Kaijima [6]).

Force-flow visualization produces intuitive and instructive topologies; moreover, it can approximate the optimal topology for a given design boundary. The research traces its roots to classical studies on structural optimization by Michell, who formulated the analytical derivation for several well-known optimal truss structures [7]. While Michell was not explicitly considering principal stress trajectories, his results closely resemble the principal stress lines for the design domain he examined, as Figure 1.0

shows. Figure 1.1 and Figure 1.2 furthermore demonstrate the typical convergences between the optimal topologies suggested by conventional computationally-intensive numerical optimization procedures (such as the ground structure and homogenization methods), and the principal stress line generated for the same design domain. These recurring resembles results suggest the potential value of a more direct approach for topological optimization that uses principal stress analysis.

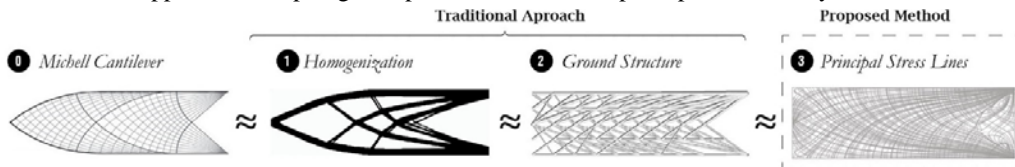


Figure 1: Convergence of optimization results to principal stress lines

To motivate the case for topology-filament alignment in AM that is based on stress line topologies, a shell geometry discretized with a grid-based and stress-line-based topology is presented in Figure 2. Analysis found the latter typology to be 20% more structurally efficient than the former typology.

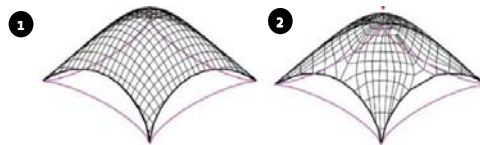


Figure 2: 4-support grid shell with: (1) Grid-based topology (2) Stress-line-inspired topology

2.1 Suitability of stress line methods in additive manufacturing

This section outlines the fundamental properties of stress lines that render stress-line-based topologies highly compatible with additive manufacturing of structurally-performative design prototypes by FDM. Structurally, given a design domain for a finite system of isotropic material operating within the elastic range, the following structural properties must also hold, as documented by Chen and Li [8]:

- 1) Stress lines are not affected by the scaling of material stiffness and applied forces.
- 2) Principal stress fields are affected primarily by attributes of the geometry of the design boundaries, and the location and degree of fixities of the loading and support conditions respectively.

These properties establish stress line techniques as geometrically-focused methods of structural evaluation, and validate the theoretical capacity for stress-line-based topologies to achieve accurate and scaled representation of the structural behavior in the printed specimen, regardless of the dimension and material properties of the final represented structure. Additionally, stress line fields can be characterized by a number of geometric properties stemming from the continuous stress distribution assumed for continuum structure operating within elastic range:

- 1) Stress lines of one principal direction for a given design domain form a continuous contour field.
- 2) Stress lines either traverse from one design boundary to another, or they may be entirely periodic.

The two geometric properties supports the logistical feasibility for the direct adaptation of stress lines as printing trajectories in FDM application, which is also a process based on the linear aggregation of tool paths. Both properties contribute to the consistent and parallel-like deposition of stress lines that avoids entanglement within each layer, and the efficient linkage of stress lines to form the printing paths.

2.2 Stress lines in digital fabrication

Recent emergence of structural analysis tools within common design platforms, such as Karamba 3D (Preisinger [9]) and other similar plug-ins, have created an environment favorable for the development of stress-line-based techniques in conceptual structural design, and in rapid prototyping technologies. In computation, Chen and Li addressed the well-known fabrication impracticality of optimum-like topologies, which theoretically contain an infinite number of members, by proposing a selection algorithm that incrementally densifies a Michell-like structure while ensuring consistent iterative gains in structural efficiency. Similarly, Michalatos and Kaijima developed robust stress line processing techniques that enables the scaling of principal stress lines according to a gradient input [6].

While structurally-oriented researchers have contributed to the computational development of stress line research, the actual materialization of stress lines in digital fabrication has been mainly led by design-oriented practitioners, whose motivation for stress-line inspired topologies may largely be aesthetic. Design projects that attempted to synthesize AM with stress line techniques include the Institute for Computational Design (ICD)'s Leichtbau BW Installation, which uses stress line analysis to inform the layout for carbon fiber reinforcing [10]. In other areas of digital fabrication, Freidmen *et al.* used principal stress lines to inform custom robotic metal sheet forming [11], as shown in Figure 3.



Figure 3: Stress-line-based fabrication: (1) Leichtbau BW Installation [10]; Robotic Bead Rolling [11]

Recognizing that the materialization of structural patterns has often been relegated to a symbolic role without much structural substantiation, and that integration of stress-line-based digital fabrication has largely been unique occurrences specialized to particular projects, this paper seeks to develop a preliminary standardized and integrated software and hardware framework that will allow designers to produce high-quality, and structurally-performative prints for a given 2.5-D surface with the use of conventional design and analytical software tools and common electronic devices.

3. Methodology

3.1 Design, analysis, scope, and case studies

To maximize the design potential of the proposed framework, the research presented on this paper is developed using the popular 3D modeling tool Rhinoceros 3D, within the parametric visual programming language environment of Grasshopper 3D. Structural analyses were conducted using the plug-in Karamba on a surface design that was initially form-found using Kangaroo Physics [12].

The implementation demonstrated in this paper focuses on form-found 2.5D membrane structures. Since these systems are subjected only to in-plane stresses, normal stresses in discretized members is primarily purely axial with negligible bending. Particularly, the proposed framework is implemented

on a basic form-found grid shell with 4 supports, as demonstrated in Figure 4.1 and Figure 4.2. Figure 4.3 shows the form-found surface milled from a wood block consisted of laminated MDF layers, in order to create the print surface that holds the extruded filament.

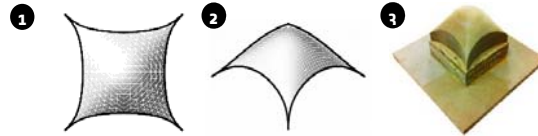


Figure 4: (1)-(2) Plan and axonometric view of the 4-support grid shell; (3) MDF-based print surface

3.2 Stress-line computation for generation of printing paths

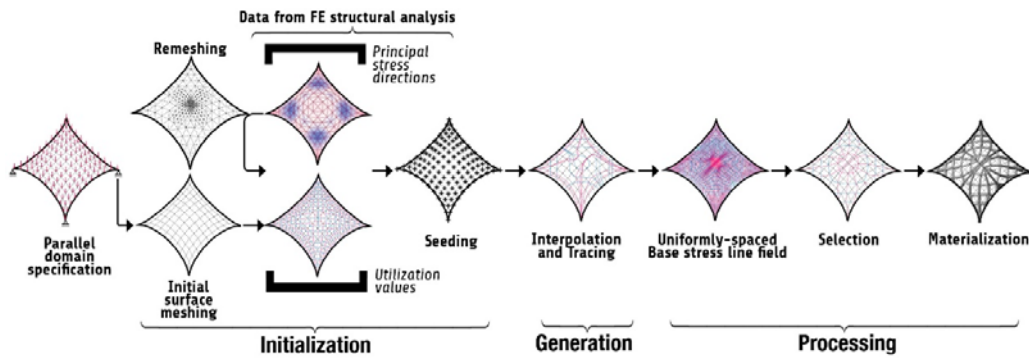


Figure 5: General stress-line-based design framework outline

The generation of stress lines follows the general methodology outlined in previous research, where the fundamental procedure for stress line generation has been broken into the three stages of initialization, generation, and processing [13], as shown in Figure 5. The purpose of initialization is to characterize the design domain with proper meshing, to conduct structural analysis on the design domain to obtain data needed for stress line construction, and to create an appropriate seeding plan from which stress lines are traced. In generation, the principal stress trajectories are extracted and materialized using enhanced interpolation method and a tracing algorithm that seeks to improve the accuracy and usability of stress line results. Once a uniformly-spaced base stress line field is obtained, the procedure concludes with strategies for processing and selecting the stress lines for materialization. Where this paper departs from the previous research on stress lines generation is the criteria that were used for stress line selection, which has been adapted here specifically for additive manufacturing, and to balance several contradicting structural, fabrication and architectural objectives that are tied to global density of stress lines to be materialized.

While structural considerations tend to favor the global densification of the stress-line-based topology to improve structural strength, aesthetic preferences may seek to enforce a minimum average spacing between stress lines in order to maintain clear articulation of the stress lines. From a fabrication perspective, excessive density can also lead to undesirable localized deposition of filament, due to the

tendency for stress lines to converge in certain junctions. In view of these concerns, a hybrid selection approach was adopted: the stress line density for each principal stress direction was optimized according to strain energy minimization, subjected to a maximum total print length and a spatial constraint that required the density of the stress lines to achieve a consistent maximum spacing between adjacent stress at 7mm, or 4x the filament diameter. The approach ensures reasonably optimal structural performance while maintaining clear topological articulation. Following selection, the stress lines were modified with rules-based corrections to improve filament extrusion ease. Example of rules include the removal of line segments in area with significant stress line overlap (See Figure 6.3).

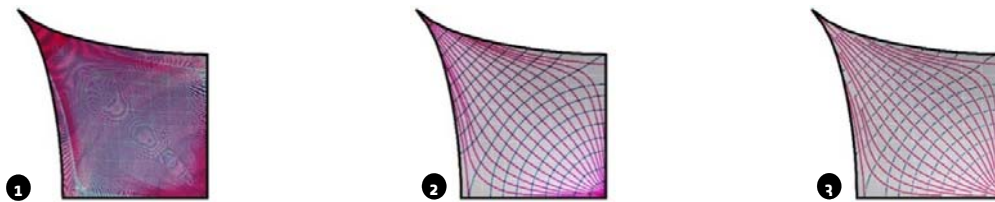


Figure 6: Additive-manufacturing-specific stress line processing: (1) Initial uniformly-spaced base stress line field; (2) Stress line density calibration; (3) Correction of stress lines for fabrication

3.3 Digital fabrication processes

This project uses the *KUKA KR6 R900 sixx* small robot. Figure 7 illustrates the fabrication work space, where the KUKA robot is centrally located inside a contained envelop. The customized heated filament extruder is pneumatically sealed to the KUKA and the MDF-based surface printing bed is clamped to the metallic work table at an eccentricity from the robot to reduce joint rotational issues.



Figure 7: Fabrication shop workspace for KUKA operation and filament extrusion

3.3.1 Custom extruder

The custom extruder is composed of a waterjet-cut aluminum frame that is mechanically coupled to the robot via a pneumatic tool changer. The aluminum frame holds a commercially available extruder sold by Signstek and control electronics. The Signstek extruder accepts 1.75mm PLA (polyactic acid, a common 3D printing material) plastic and is composed of a 1.8 degree stepper motor, heating element, thermistor, and cooling fan. Using an Arduino Uno microcontroller (Kushner [14]) and a N Type MOSEF, the closed loop temperature control (PWM) of the extruder nozzle was utilized. The KUKA's 24V signal outputs were monitored by the onboard Arduino and were used to start and stop the stepper motor/extrusion. Control of the stepper motor was achieved with an EasyDriver board that uses an Allegro A3967 motor driver chip. Details of the extruder are shown in Figure 8.

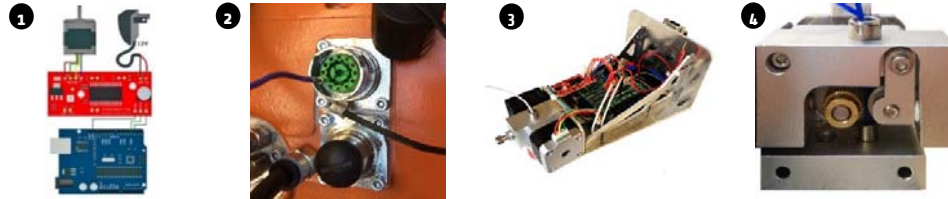


Figure 8: (1) Schematic wiring diagram, (2) Communication between KUKA and Arduino through digital pin manipulation, (3) Custom extruder module, (4) Signstek extruder with fan removed

3.3.2 Workflow and software programming interface

The KUKA KR6 Robot arm is programmed with KRL code, and the robot instructions are generated in RobotMaster [15], which is a plugin to MasterCAM [16]. The typical workflow consists of the following iterative and trial and error procedure: 1) Import of print surface and stress line data from CAD into CAM software; 2) Specimen positioning in the workspace; 3) Print surface calibration in the CAM model space; 4) Clustering of paths based on robot work volume and reach limitations; 5) Assigning stress-line-based geometry for toolpath generation; 6) Iteration of possible joint configurations in CAM and RobotMaster interface; 7) Optimization and simulation of robot trajectory; and 8) Export KRL code and run program in KUKA.

3.3.3 Key robot movement parameters

The subsection describes parameters that are key determinants to the quality of the printed filament.

Offset: To ensure a consistent quality in the printed filament and improved adhesion between filament and print surface, the offset between the nozzle and the printed surface is set at a level to allow the tip of the nozzle to drag along the top of the extruded filament uniformly across a stress curvature.

Extrusion activation timing: To mitigate the loss of filament due to a residual pressure gradient across the nozzle and to ensure the production of normalized flow at the start of new stress-line-based paths, the filament is retracted immediately after the end of a tool path to break connection with the previous filament, and extruded again just prior to recommencing print for the following stress line.

Travel and move rate: The robot's movement is measured by its move rate, which differs from the actual travel rate of the extrusion tip over the print surface due to rotational requirement of the joints that are specific to the geometries of each stress-line-based path. Typically, decrease in the travel rate corresponds to the thickening of the deposited material, whereas increases may cause poor adhesion.

Tool axis orientation: Generally, there are two types of surface tool axis orientation: 5-axis maintain complete normalcy and 4-axis maintain normalcy only in one axis. 5-axis setting achieve the greatest consistency in the filament's cross section profile, thus leading to the best aesthetic and structural performance. However, 4-axis settings can be used when joint rotational and collision issues prohibit stress-line-based paths to be printed at complete normalcy.

3.3.4 Paths clustering, assignments, sequencing, and print program generation

The generation of the individual print programs begins with the selection and linkage of the stress-line-based paths. Due to robot work volume and reach limitations, it is generally difficult to extrude paths in

a single print. Thus, stress-line-based paths are clustered into a series of separate print programs, with the print surface likely rotated at least once throughout the procedure. Reasonable estimation of the KUKA arm's limitation guides the global clustering of stress lines corresponding to different print surface orientation, whereas geometric similarities guide the clustering of stress-line-based path internal to each surface orientation (see Figure 9.1 and Figure 9.2). Next, the stress lines assigned to each cluster are linked, and sequenced in a way that minimizes the KUKA's total travel distance. Conventionally, this leads to a zigzagging linkage pattern connecting the end points of adjacent stress lines, as seen in Figure 9.3.

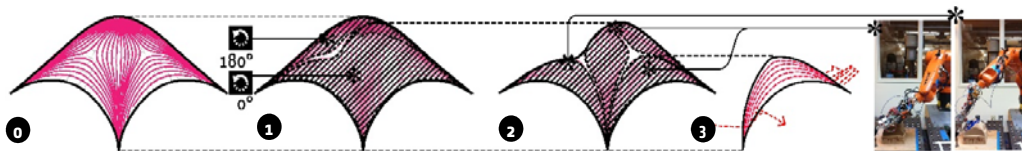


Figure 9: Process to convert stress-line-based paths into print programs: (0) Stress lines within one layer, (1) Global clustering according to print surface orientation, (2) Local clustering by geometric and robot movement consideration, (3) Sequencing/linkage of stress-line-based paths

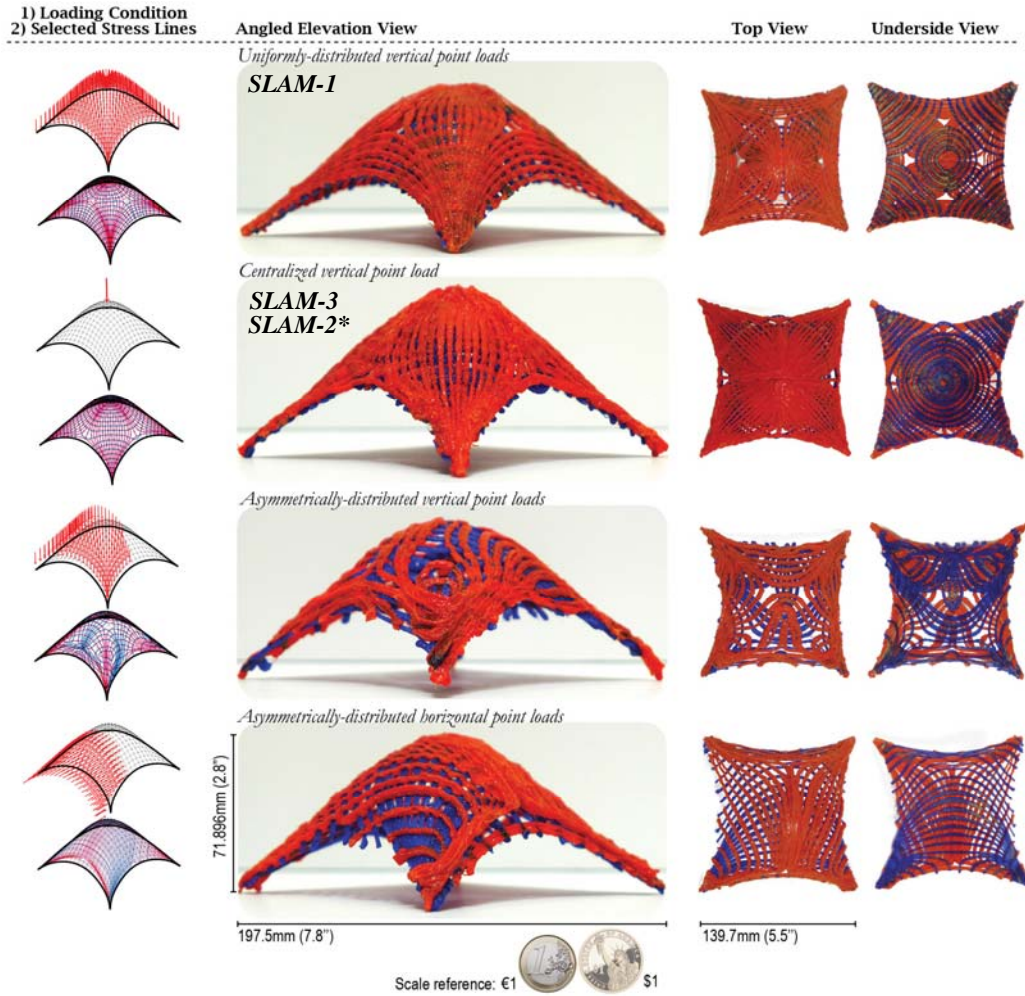
Following the assignment and sequencing of paths is the initial automated generation and simulation of the KUKA's movement trajectory. Additional iterative optimization within the robot programming interface can resolve singularity, collision, and joint limit issues that can remain in the initially generated trajectory. Once a satisfactory movement is obtained, the print program is exported as KRL code, and loaded into the KUKA robot to commence the printing procedure.

4. Results

4.1 Fabrication results

Based on the SLAM methodology described in the previous section, several small-scale specimens were fabricated for the four-support shell structure introduced in Figure 4. While in all cases, a uniform load was used to generate the global shell geometry, different loading cases were used to generate stress-line-based structural topologies for printing with the SLAM method, as follows: 1) uniformly-distributed vertical load 2) centralized vertical point load 3) asymmetrically-distributed horizontal load, and 4) asymmetrically-distributed vertical load. The resulting specimens produced from these load cases are shown in Figure 10. It is noteworthy that in a real end-use application, several layers of stress lines based on different loading conditions could be superimposed to create a resilient structure.

The images in Figure 10 show that the SLAM methodology is relatively successful at achieving complex, structurally meaningful geometries and topologies for 2.5-D surface structures. There is some degree of imperfection, imprecision, and variability that could be reduced as the process is further standardized and improved; there is also some mold release difficulty evident in the MDF material adhering to the bottom of some shells. The resulting structures are stiff to the touch and appear to have sufficient bonding between the overlapping orthogonal printed lines. The structural performance of these results is further validated in the following section, which presents structural load testing results.



*SLAM-2, which is not shown here, has the same topological connectivity as SLAM-3, but with variable filament width.

Figure 10: Fabrication results of stress-line-based topologies for various loading cases

4.2 Structural load testing results

To validate that SLAM-produced specimens perform better than conventionally 3D-printed parts, a comparative load test was completed on five specimens: three printed using the SLAM method, and two printed using a conventional layer-based 3D printer (MakerBot). Both methods use the same material (PLA plastic), and an attempt was made to standardize the material volume in each sample. The MakerBot specimens were printed as solid, constant-thickness shells. Details about the five specimens

are summarized in Table 1. The specimens were structurally tested using a single centralized vertical point load, which was applied until a peak load was reached (generally beyond an initial failure). Figure 11 shows images of the load testing, and Figure 12 shows a normalized load-displacement plot.

Specimen Name	<i>SLAM-1</i>	<i>SLAM-2</i>	<i>SLAM-3</i>	<i>MB-1</i>	<i>MB-2</i>
Filament Orientation	Distributed load stress lines	Point load stress lines	Point load stress lines	Horizontal	Horizontal
Filament Thickness	Constant	Varies with stress	Constant	N/A	N/A
Mass [g]	40.7	49.9	53.5	39.3	40.2
Ultimate Failure Load [N]	1385	1515	1449	735	866
Normalized Failure Load [N/N]	3468	3101	2762	1907	2198
Failure Mode	Filament crushing/bending, global fracture	Filament crushing/bending,	Filament crushing/bending,	Intra-layer bond	Intra-layer bond
Failure Profile	Ductile	Ductile	Ductile	Brittle	Ductile

Table 1: Data and results for five specimens used in structural load testing

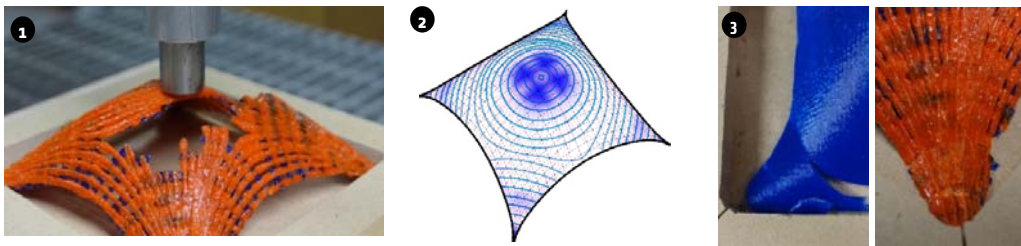


Figure 11: (1) Load testing failures, (2) Tension in minimum principal plane, with stress magnitude corresponding to color intensity, (3) Conventional MB specimen failing in bond between layers.

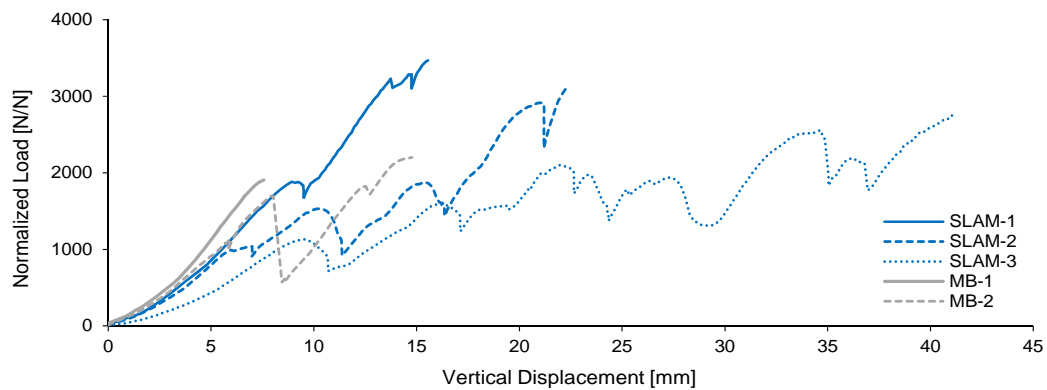


Figure 12: Normalized load vs. displacement plot of five load-tested specimens

While the number of tests conducted is not high enough to be statistically conclusive, these preliminary results suggest that the SLAM method does lead to improved structural behavior compared to conventionally 3D-printed parts. The main structural benefits are improved strength (i.e. failure load) and ductility after initial failure. There is no improvement in stiffness, which makes sense since the SLAM method does not change global geometry or material (this result is also supported by previous research, Mueller *et al.* [17]). In the MakerBot specimens, failures occurred in the shell where tensile stresses were predicted to occur in FEA, as shown in Figure 11.2, although there was not significant tension expected for this geometry and loading. More significant advantages for the SLAM method would be expected for geometries and loadings that induce more tension.

5. Conclusions

5.1 Future work

There are several important directions for future work in SLAM. First, fabrication methods should be consolidated to reduce variability in the quality of printed product, so that results can be consistently reproduced. There is also a need to conduct a robust investigation on the various robot programming parameters discussed in this paper, in order to ascertain the relationship between their variations and the structural performance of the printed specimen. The knowledge is crucial to the long-term objective of developing SLAM techniques into a viable and accurate structural prototyping tool, and for end-use structures. Regarding robotic programming, future work should develop more intelligent, robust and automated methods of path generation that permit local parameter variations within each stress-line-based paths. This may require the adoption of an alternative robot programming platform that allows for custom programming: preliminary investigations have been explored using the Grasshopper plugin HAL. Consolidating the workflow within a single robust computational environment will generate productivity gains, and allow for robot movement that is closely adapted to the geometric and structural properties of respectively the print surface and the stress-line-based topology. Finally, there is potential to expand the hardware capability of the extrusion module: for example, sensors can allow extrusion parameters to vary according to the conditions of the printed surface.

5.2 Final remarks

The research pursued in this paper constitutes a promising first step in validating a new approach to AM that simultaneously capitalizes on multi-axis machining capability and satisfies structural objectives. Thus, this work contrasts with recent developments in AM technologies that are focused mostly on improving free-form extrusion capability; this paper's incorporation of principal stress line techniques ensures that printed specimens will achieve both geometrical fluidity and structural capacity. Moreover, structural load testing was able to verify that the proposed method outperforms methods using the conventional layer-based paradigm, while the experiments have also provided valuable insights on structural behaviors that are particular to oriented material deposition techniques. The most important contribution, however, is the articulation of a consolidated methodology that encompasses structural analysis, topological generation, fabrication of extrusion module, and machine programming: this research has demonstrated the feasibility of a new AM technique that can empower designers to fabricate structurally-performative and geometrically-compelling 2.5-D surface designs.

Acknowledgements

The authors wish to thank the following students who assisted with various aspects of this research: Jonathan Mackaman, Akshat Bubna, Elizabeth Bianchini, Katie Gertz, Colin Poler, Xinyi Ma. Additionally, the authors acknowledge MIT fabrication lab coordinators Justin Lavallee, Chris Dewart, Jen O'Brien, shop monitors Inés Ariza and James Addison, and testing lab guru Stephen Rudolph.

References

- [1] Mueller C., Irani A. and Jenett B. Additive Manufacturing of Structural Prototypes for Conceptual Design, in *Proceedings of the International Association for Shell and Spatial Structures (IASS) Symposium*, 2014.
- [2] Gibson I., Rosen D. W. and Stucker B., *Additive Manufacturing Technologies*, Springer, 2010
- [3] Contour Crafting, from: <http://www.contourcrafting.org/>, access date: May 2015.
- [4] 3D Print Canal House, from: <http://3dprintcanalhouse.com/>, access date: May 2015.
- [5] Joris Laarman Lab. MX3D_Resin, from: <http://www.jorislaarman.com/mx3d-resin.html>, access date: May, 2015.
- [6] Michalatos P. and Kaijima S., Eigenshells: Structural patterns on modal forms, in *Shell Structures for Architecture: Form Finding and Optimization*, Adriaenssens S., Block P., Veenendaal D. and Williams C. (ed.), Routledge, 2014, 195-210.
- [7] Michell A.G.M., The Limits of Economy of Material in Frame-Structures. *Philosophical Magazine* 1904; 47(8); 589-97.
- [8] Chen Y. and Li. Y., Beam Structure Optimization for Additive Manufacturing based on Principal Stress Lines, in *Solid Freeform Fabrication Proceedings*, 2010.
- [9] Preisinger C. Karamba, from: <http://www.karamba3d.com/>, access date: May, 2015.
- [10] Institute for Computational Design. Leichtbau BW Installation, Hannover Fair 2014, from: <http://icd.uni-stuttgart.de/?p=10941>, access date: May, 2015.
- [11] Fiedman J., Hosny A. and Lee A., Robotic Bead Rolling - Exploring Structural Capacities in Metal Sheet Forming, in *Robotic Fabrication in Architecture Art and Design*, McGee W. and Ponce de Leon M. (ed.), Springer, 2014, 83-98.
- [12] Piker, D., Kangaroo: Form Finding with Computational Physics. *Architectural Design* 2013; 83(2); 136-37.
- [13] Tam, K.M.M., *Stress Line Computation for Discrete Topological Generation*, Master's thesis, Massachusetts Institute of Technology, May 8, 2015.
- [14] Kushner. D. The Making of Arduino – How five friends engineered a small circuit board that's taking the DIY world by storm, from: <http://spectrum.ieee.org/geek-life/hands-on/the-making-of-arduino>, access date: May, 2015.
- [15] Jabez Technologies. RobotMaster – CAD/CAM for Robots, from: <http://www.robotmaster.com/>, access date: May, 2015.
- [16] CNC Software, Inc. Mastercam, from <https://www.mastercam.com/en-us/CompanyInfo>, access date: May, 2015.